韓國鑛物學會誌 第 6 卷 第 2 號(1993)
J. Miner. Soc. Korea, 6, 105－115(1993)

Mössbauer and Infrared Absorption Spectroscopy of Tourmaline Minerals

전기석 광물의 뫼스바우어 및 적외선 흡수 분광학

Hee Jong Kim (김희종) · Soo Jin Kim (김수진)

Department of Geological Sciences, Seoul National University, Seoul 151-742, Korea
(서울대학교 지질과학과)

ABSTRACT : Mössbauer and Infrared absorption spectra of the iron-bearing tourmaline minerals show that the ferrous and ferric ions occupy the Y and Z octahedral sites. The Fe ions are almost ferrous, predominantly partitioning into Y site and partly take in Z site. The Fe^{2+} content of the Z sites in brownish black tourmaline minerals are higher than that in blue/green tourmaline minerals. Therefore, 720 nm peak of brownish black samples is broader than that of blue/green samples in optical spectra. All of the blue/green tourmaline minerals used in experiment have only Fe^{2+} ion.

The IR spectra of tourmalines depend on the cation environments around OH groups, as also evidenced by their chemical analyses. There appear no difference in IR spectrum between O(1)H and O(3)H bonding characters in the heat-treated samples. But the characteristic 3565 cm^{-1} peak appears in the ferrous hydroxyl bearing silicates, where dehydroxylation temperature for OH coordinated to Fe^{2+} is 700～800 ℃.

요약 : 철을 함유하는 전기석 광물들의 뫼스바우어 및 적외선 흡수 스펙트럼들은, 철 2가와 철 3가 이온들이 Y와 Z팔면체 자리에 들어가는 것을 보여준다. 철 이온들은 대개 2가인데, 대부분 Y자리에 분포되며 부분적으로 Z자리에도 들어간다. 흑갈색 전기석 광물들은 청색/녹색 전기석들 보다 Z자리의 철 2가 성분이 높다. 그러므로, 광학 스펙트럼으로 보면 흑갈색 전기석의 720 nm피크가 청색/녹색 전기석의 피크보다 더 넓게 나타난다. 실험에 이용된 녹색/청색 전기석 광물들은 모두 철 2가 이온들만 가지고 있다.

전기석들의 적외선 스펙트럼들은 화학 분석결과로 보아 OH 주위의 양이온들의 환경에 따라 민감한 변화를 보인다. 열처리한 시료의 분석결과를 보면, O(1)H와 O(3)H의 적외선 흡수 스펙트럼 특성에는 차이를 보이지 않았다. 철 2가와 OH를 가지는 규산염 광물의 경우, 3565 cm^{-1} 피크를 특징적으로 가지는데 이들의 탈수온도는 700～800 ℃이다.

INTRODUCTION

Tourmaline is a borosilicate with general formula $XY_3Z_6(BO_3)_3Si_6O_{18}(OH)_4$ and space group R3m (Wilkins et al., 1969). The X site is usually occupied by large cations such as Na^+, K^+, Ca^{2+}, while the Y site by smaller cations such as Li, Al, Fe^{2+}, Fe^{3+}, Mg, and Mn^{2+}. The Z site is chiefly occupied by Al, but Al can be replaced by Fe^{3+}, Cr^{3+}, V^{3+} (Barton, 1969). Because of a wide substitution in Y site, tourmaline minerals usually have end member: dravite, schorl, and elbaite with Mg, Fe, and (Li, Al) in the Y position, respectively.

Absorption bands in the OH stretching region of infrared spectra vary with the nature of the

cations directly coordinated to OH. The OH groups can occupy two different positions; at the center of hexagonal rings O(1)H and the border of the brucite-like fragments O(3)H. The OH groups in the last position are electrostatically perturbed by tetrahedral oxygens and are three times more numerous than those placed in the first position (Vedder, 1964; Strens, 1974; Rausell et al., 1979; Gonzalez-Carreno, 1988). The present study aims to characterize Mössbauer and infrared absorption spectroscopic properties of tourmaline minerals.

MATERIALS AND METHODS

The majority of brownish black tourmaline samples were obtained from Uncheon and Haksan mines in Korea and San Diego mine in California, U.S.A. and blue/green tourmaline samples from anonymous mine in Brazil.

The studied tourmaline specimens were described by Kim and Kim (1993). Experimental details and analysed data of these minerals are the same as those reported by them.

Mössbauer resonance spectra of tourmaline minerals were recorded on a constant acceleration ASA (Austin Science Associates) S600 Mo ssbauer spectrometer using 1024 channels of a nuclear data multichannel analyzer with Co source in a rhodium matrix (10 mCi) in the Department of Physics, Yeungnam University.

The purified samples were ground with acetone so as to prevent Fe ions from oxidizing. The sample was mounted in a holder with a round hole (2 cm in diameter) and run at 80 K, 300 K, and 1070 K. Low temperature experiment was performed in He gas and high temperature experiment in air. Centroed shifts are given relative to metallic Fe. Each spectrum was accumulated for over 1-2 days to acquire at least 6×10^5 counts of baseline per channel for the good statistics within the velocity range of about 7.32 mm/sec and calibrated relative to metallic Fe foil.

The Mössbauer spectra were transferred to computer to execute curve-fitting calculations and to plot the simulated curve. For curve fitting, the program employed the Gauss non-linear regression method, assuming Lorenzian curve shapes with various parameters.

Infrared absorption spectra were obtained on the doubly polished plates and the polished thin sections using a Bomen Da-3 FTIR spectrophotometer at Inter-University Center for Natural Science Research Facilities in Seoul National University. IR absorption spectra were recorded in 3800~3300 cm^{-1} range and measured at 1cm $^{-1}$ resolution using liquid-nitrogen cooled MCT (HgCdTe) detectors. IR spectra were obtained for heat-treated samples in furnace. Temperature was raised from 300 to 900 ℃ by increasing 100 ℃ per each day for the first three days and 100 ℃ every two days for the next eight days.

RESULTS AND DISSCUSION

Mössbauer Spectroscopy

Mössbauer data for a few Li, Al-tourmaline minerals show very low or undetectable Fe^{3+} (Burns, 1972; Simon, 1973; Faye et al., 1974). Most Mössbauer studies have focused on Fe, Mg-tourmaline minerals and have detected much larger and quite variable Fe^{3+} contents (Hermon et al., 1973; Gorelikova et al., 1976; Saegusa et al., 1979). Ferrous/ferric ratios and site occupancies of iron cations in tourmaline minerals have been determined from Mössbauer analysis. We could get not only the evidence of Fe^{3+} ions in the two octahedral sites, but also unequal distributions of Fe^{2+} in both octahedra. The excited nuclear state is shifted from zero energy due to d-electron shielding effects on s-electron density and is split into a quadrupole doublet due to asymmetric electronic environments (electric field gradient)

Table 1. Mössbauer parameters of brownish black tourmalines at different temperatures.

	K1		statistical error:		2.25
T(K)	I.S	Q.S	HWHM	AREA(%)	ASSIGNMENT
	0.26	0.86	0.29	20.02	Fe^{3+}(Y)
300	0.61	1.26	0.18	19.20	$Fe^{2.n+}$
	0.86	1.36	0.23	18.62	$Fe^{2.n+}$
	1.02	2.37	0.19	42.18	Fe^{2+}(Y)
	0.30	0.94	0.28	16.22	Fe^{3+}(Y)
80	0.55	1.18	0.22	8.78	$Fe^{2.n+}$
	1.04	1.71	0.22	18.12	$Fe^{2.n+}$
	1.09	2.54	0.20	56.88	Fe^{2+}(Y)
	K2		statistical error:		1.13
T(K)	I.S	Q.S	HWHM	AREA(%)	ASSIGNMENT
	1.03	2.45	0.13	54.16	Fe^{2+}(Y)
300	0.99	2.09	0.18	30.26	Fe^{2+}(Z)
	0.94	1.48	0.22	15.58	$Fe^{2.n+}$
80	1.34	2.63	0.14	50.16	Fe^{2+}(Y)
	1.12	2.32	0.26	49.84	Fe^{2+}(Z)
	AB1		statistical error:		1.24
T(K)	I.S	Q.S	HWHM	AREA(%)	ASSIGNMENT
	1.04	2.43	0.15	63.72	Fe^{2+}(Y)
300	0.99	2.26	0.14	4.48	Fe^{2+}(Z)
	0.98	1.70	0.27	31.82	$Fe^{2.n+}$
	1.10	2.60	0.15	68.08	Fe^{2+}(Y)
80	1.09	2.26	0.16	20.32	Fe^{2+}(Z)
	1.06	1.79	0.23	11.60	$Fe^{2.n+}$

* I.S: Isomer shift (mm/s)
* Q.S: Quadrupole splitting (mm/s)
* HWHM: Half width at half maximum (mm/s)
* $Fe^{2.n+}$ refers to the non-integral iron where the extra electron is delocalized.

(Korosssvushkin, et al., 1979; Mattson, et al., 1984).

Mössbauer effect spectra of tourmaline and its H_2 annealed product were obtained at two different temperatures of 80 and 300 K. The results from the computer fits are shown in Tables 1 and 2, and Figures 1 and 2. In the Figures, only the high velocity components of the absorption doublets are resolved. Annealing in hydrogen inhibits the electron delocalization and forces the itinerant electron to be localized in one of the two

Table 2. Mössbauer parameters of blue/green tourmaline minerals at different temperatures.

	BG2		statistical error:		1.42
T(K)	I.S	Q.S	HWHM	AREA(%)	ASSIGNMENT
300	1.02	2.39	0.16	91.98	Fe^{2+}(Y)
	1.05	1.85	0.17	8.02	Fe^{2+}(Z)
80	1.12	2.45	0.20	90.90	Fe^{2+}(Y)
	1.25	2.15	0.18	9.10	Fe^{2+}(Z)
	B7		statistical error:		2.12
T(K)	I.S	Q.S	HWHM	AREA(%)	ASSIGNMENT
300	1.02	2.37	0.16	88.96	Fe^{2+}(Y)
	1.04	1.98	0.21	11.04	Fe^{2+}(Z)
80	1.12	2.46	0.20	91.20	Fe^{2+}(Y)
	1.17	1.97	0.21	8.80	Fe^{2+}(Z)
	BG1		statistical error:		3.22
T(K)	I.S	Q.S	HWHM	AREA(%)	ASSIGNMENT
300	1.36	2.35	0.19	96.75	Fe^{2+}(Y)
	1.71	1.74	0.08	3.25	Fe^{2+}(Z)
	BG4		statistical error:		1.12
T(K)	I.S	Q.S	HWHM	AREA(%)	ASSIGNMENT
300	1.36	2.39	0.16	91.08	Fe^{2+}(Y)
	1.46	1.98	0.13	8.92	Fe^{2+}(Z)
	BG6		statistical error:		1.19
T(K)	I.S	Q.S	HWHM	AREA(%)	ASSIGNMENT
300	1.35	2.38	0.16	95.36	Fe^{2+}(Y)
	1.58	2.04	0.08	4.64	Fe^{2+}(Z)

* I.S: Isomer shift (mm/s)
* Q.S: Quadrupole splitting (mm/s)
* HWHM: Half width at half maximum (mm/s)
* $Fe^{2.n+}$ refers to the non-integral iron where the extra electron is delocalized.

octahedral sites. This results in iron of integral valence states (Fe^{2+} and Fe^{3+}), while the total oxidation ratio remains constant. This ordering of Fe^{3+} in the Y site and Fe^{2+} in the Z site on an nealing in hydrogen is also observed by optical spectroscopy (Smith, 1978).

Brownish black tourmaline

The mixed site occupancies of both Fe^{2+} and Fe^{3+} ions are demonstrated by the Mössbauer spectrum of a sample K1 in Figure 1a. The

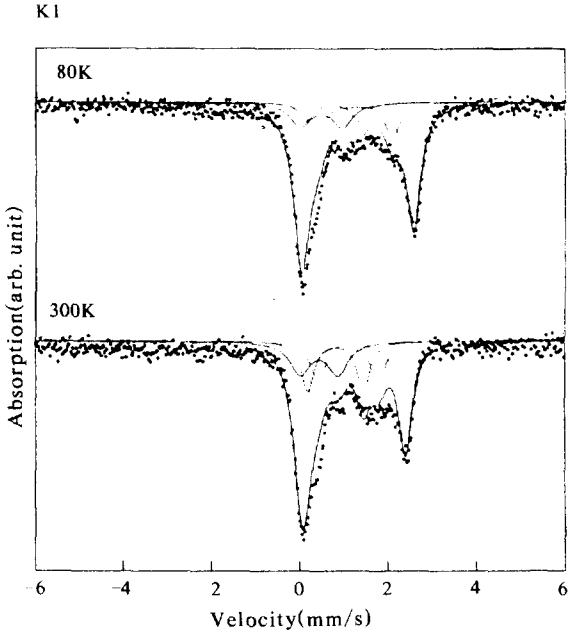

(a)

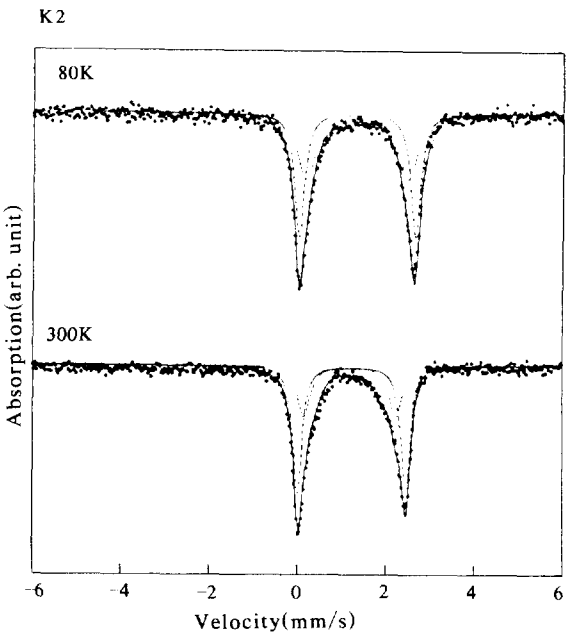

(b)

Fig. 1. ^{57}Fe Mössbauer spectra of brownish black tourmalines (samples K1, K2, and AB1) at different temperatures. A best-fit, 2 doublets calculated spectrum and components are shown for both spectra. Velocity is shown relative to sodium nitroprusside. **(a)** Upper diagram; Experiment carried out at 80 K. Iron occupies several nonequivalent sites. Lower diagram; Experiment carried out at room temperature. Iron occupies several nonequivalent sites.

Fig. 1 (continued). (b) Upper diagram; Experiment carried out at 80 K. Iron occupies two positions: Fe^{2+} in Y and Z sites. Lower diagram; Experiment carried out at room temperature. Iron occupies two positions: Fe^{2+} in Y and Z sites.

spectra obtained at 80 K and 300 K have been fitted to four doublets. The assignments, parameters, and computed areas are summarized in Table 1. The four doublets demonstrate that both ferrous and ferric ions are distributed over two six coordinated sites of tourmaline structure with significant amounts of each cation in the Y sites. The Mössbauer effect parameters (especially the isomer shift, which is sensitive to the electron density around the iron nuclei) for these three doublets indicate values that are intermediate between those of Fe^{2+} and Fe^{3+}, and are assigned to iron with non-intergral oxidation state, $Fe^{2.n+}$ (Saegusa et al., 1978). In the spectrum at 300 K (Fig. 1a), the broad envelope between the high velocity Fe^{2+} and Fe^{3+} absorption peaks is due to delocalized electrons around iron. The isomer shift (I. S) and quadrupole splitting (Q. S) of both doublets are consistent with ferric iron in an octahedral site (Table 1). Their ranges are 0.25 ~ 0.68 and 0.64 ~ 0.96, respectively (Burns, 1972; Gorelikova et al., 1976; Ferrow et al., 1988). Sample K1 unlike other samples has Fe^{3+} and its optical spectrum shows absorption peaks at 594 and 635 nm peaks. A comparison of this spectrum with that of a typical tourmaline shows the basic features of Fe^{2+}-Fe^{3+} interactions in tourmaline (Kim and Kim, 1993).

Sample K2 shows that Fe ions are all ferrous which is predominantly partitioned into Y site and partly take in Z site (Table 1). The Fe^{2+} contents of the Z sites in brownish black tourmaline minerals are higher than that in blue/green tourmaline minerals. Therefore, 720 nm

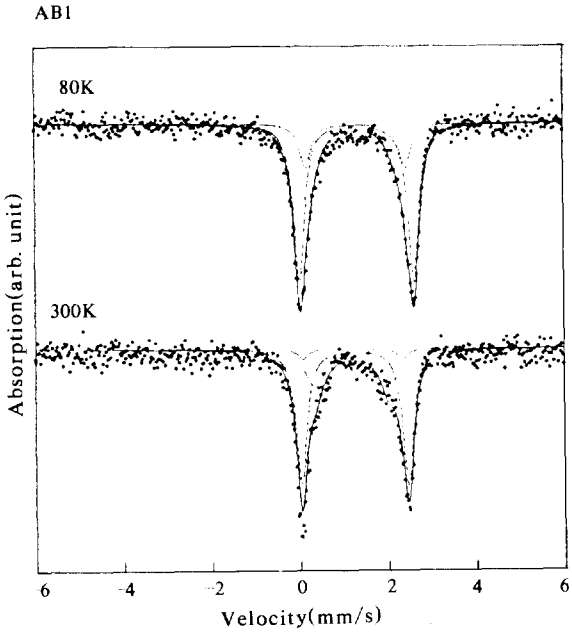

(c)

Fig. 1 (continued). (c) Upper diagram; Experiment carried out at 80 K. Iron occupies nonequivalent sites. Lower diagram; Experiment carried out at room temperature. Iron occupies several nonequivalent sites.

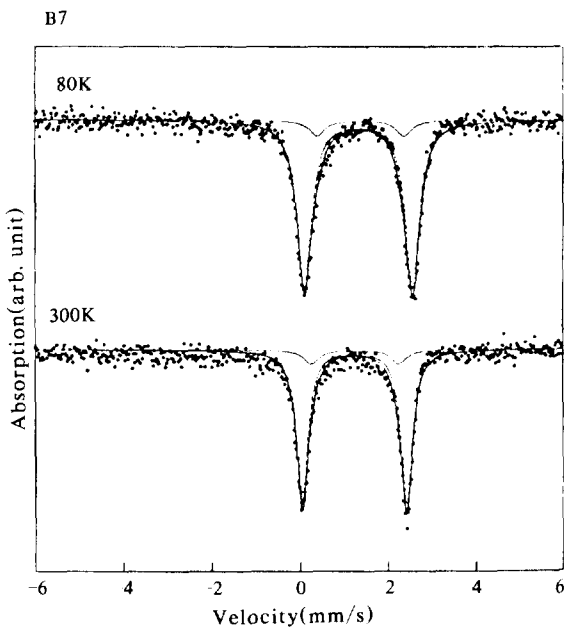

(a)

Fig. 2. ^{57}Fe Mössbauer spectra of blue/green tourmalines (Samples B7, BG1, BG4, and BG6) at different temperatures. A best fit, 2 doublets calculated spectrum and components are shown for both spectra. Velocity is shown relative to sodium nitroprusside. (a) Upper diagram; Experiment carried out at 80 K. Iron occupeis two positions: Fe^{2+} in Y and Z sites. Lower diagram; Experiment carried out at room temperature.

peak of sample K2 is broader than that of blue/green tourmaline samples in optical spectra (Kim and Kim, 1993). It has been concluded that there are related between 720 nm peak and Fe^{2+} content of Z sites in Fe-bearing tourmaline minerals. The result of Mössbauer analysis of brownish black tourmaline minerals at 1070 K shows that Fe ions are ferric in all samples (Fig. 3).

Blue/green tourmaline

The mixed site occupancies of iron cations in the blue/green tourmalines of the elbaite-schorl series are demonstated by the Mössbauer spectra shown in Figure 2. Though only two peaks appear in the spectrum there is pronounced asymmetry on the inner shoulders of the peaks, indicating the presence of a second ferrous doublet with smaller quadrupole splitting. All of the blue/green tourmaline minerals used in experiment have Fe^{2+}. The outer doublet is attributed to Fe^{2+} ions in the Y sites and the inner doublet to Fe^{2+} ions in the Z sites (Burns, 1972). The computed areas indicate that the Fe^{2+} ions is predominantly partitioned into Y site and below 11% of the Fe^{2+} ions enter the Z sites (Table 2). The results of Mössbauer analysis of blue/green tourmaline minerals at 1070 K show that Fe ions are ferric in all samples (Fig. 3) and sample BG6 additionally shows the hyper fine effect unlike other samples (Fig. 4) (Table 3). In its optical spectrum, the yellowish green color changed to light green unlike other samples (Kim and Kim, 1993). Hence, it is inferred that it has different

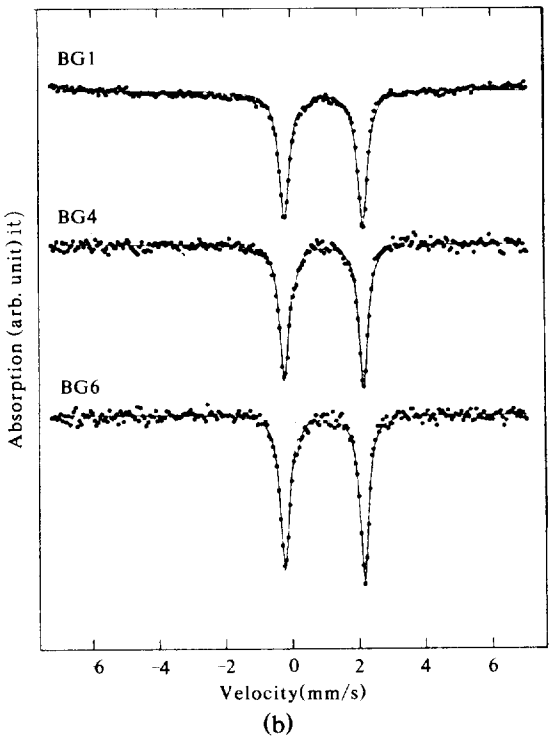

Fig. 2 (continued). (b) Experiment carried out at room temperature. Iron occupies two positions: Fe^{2+} in Y and Z sites.

proton environment compared with other heat-treated samples.

Infrared Absorption Spectroscopy

Absorption bands in the OH stretching region of infrared spectra vary with the nature of the cations directly coordinated to OH and have been used to study different cation substritutional schemes in minerals (Vedder, 1964; Strens, 1974; Rausell et al., 1979). In this work, the influence of chemical composition on the IR spectra has been studied in order to differentiate the bands associated with the different types of OH and to assign the observed infrared spectra.

IR stretching band assignment

In the structure of tourmaline, the OH groups

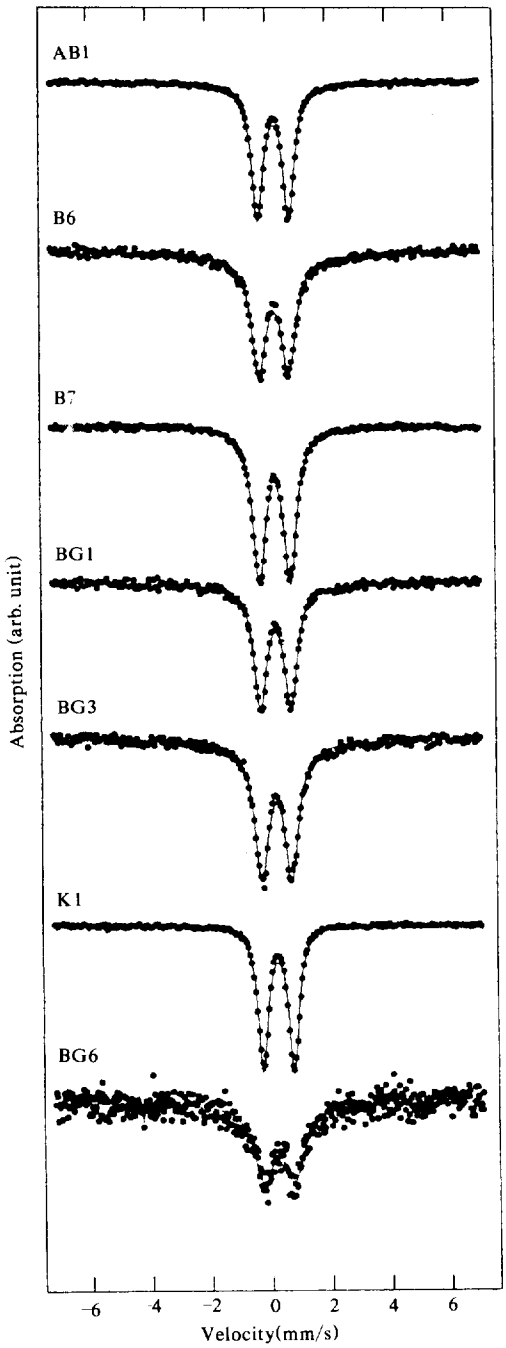

Fig. 3. ^{57}Fe Mössbauer spectra of blue/green and brownish black tourmaline minerals annealed in air at 1070 K. Velocity is shown relative to sodium nitroprusside.

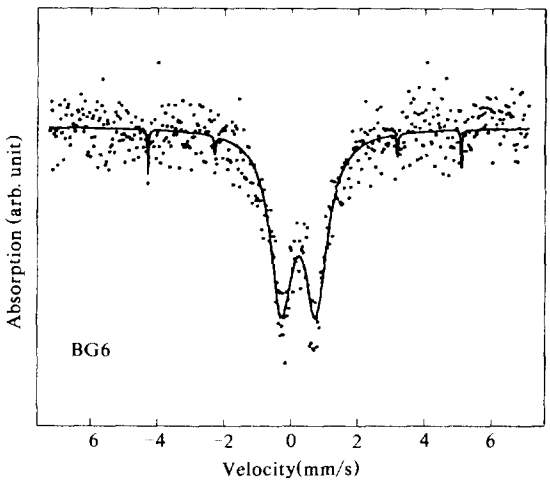

Fig. 4. This diagram is magnified BG6 of Figure 3 and shows slightly weak hyperfine effect unlike other samples.

Table 3. Mössbauer parameters of BG6 tourmaline showing hyperfine effect.

Statistical error: 1.13

T(K)	I.S	Q.S	HF	HWHM
1070	0.80	−0.04	340.34	0.00
	0.59	1.02		0.40

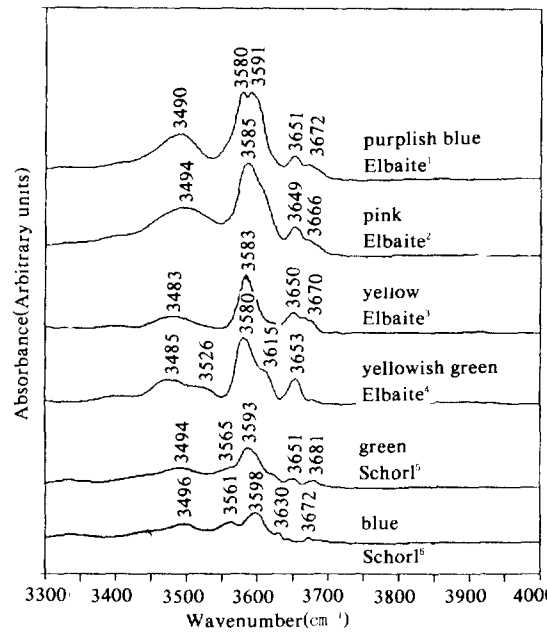

Fig. 5. Hydroxyl stretching regions of IR spectrum of various mono-colored tourmaline minerals cut // c axis.

1: sample BPB, 2: sample AP5, 3: sample AWB, 4: sample AGY, 5: sample BG3, 6: sample BG1. AP5, AWB, AGY, and BPB are Elbaite. BG1 and BG3 are Schorl.

occupy two different crystallographic positions. The first position O(1)H is located at the center of hexagonal rings and the OH is coordinated to three Y octahedral cations. The second position O(3)H is located at the border of hexagonal pillars and the OH is coordinated to two aluminiums and one Y cation. The highest frequency bands (3700~3630 cm^{-1}) in the IR spectra correspond to O(1)H located in the hexagonal rings and the bands in the region of 3600~3400 cm^{-1} correspond to O(3)H located at the border of the trigonal brucite-like fragments (Gonzalez-Carreno, 1988). The OH stretching regions (3800~3300 cm^{-1}) of IR spectra of tourmaline minerals cut // c axis are presented in Figure 5. From this Figure it is evident that IR spectra vary with composition of tourmaline and that there exist three regions of different characteristic OH bands: 1) 3700~3630 cm^{-1}, where the ranges are narrow and generally low in intensity, 2) 3600~3400 cm^{-1}, where the bands are wide and intense, and 3) 3400~3300 cm^{-1}, where bands are broad but not well resolved. Gonzalez-Carreno (1988) assigned 3583~3594 cm^{-1} to AlAlLi, 3568cm^{-1} to AlAlMg or AlAlMn, 3553~3558 cm^{-1} to AlAlFe, and 3464~3494 cm^{-1} to AlAlAl.

In the case of schorl in which the cations in Y sites are partly occupied by Mg and Fe, the infrared spectra in the regions of 3600~3400 cm^{-1} are composed of a unique absorption band at 3490 cm^{-1} and 3570~3550 cm^{-1} (Fig. 5). According to Gonzalez-Carreno (1988), dravite or schorl having over 10 wt% of R^{2+} (=Fe, Mg) shows very intensive peak in near 3560 cm^{-1} but does not show any discerniable peak near 3490 cm^{-1}. Schorl samples used in in this work (sample

Table 4. Assignment of the observed hydroxyl stretching bands (cm^{-1}) in the IR spectrum of mono-colored tourmaline minerals.

Samples	O(1)H		O(3)H		
			AlAlLi	AlAlR^{2+}	AlAlAl
Schorl[1]	FeFeMg	3681	3593	3565	3494
		3651			
Elbaite[2]	AlAlLi	3687	3585	–	3474
		3649			
Elbaite[3]	AlAlLi	3666	3585	–	3494
		3649			
Elbaite[4]	AlCuLi	3692	3591	–	3490
		3651	3580		
Elbaite[5]	AlMnLi	3666	3583	–	3483
		3650			

Notes: *; R^{2+} (=Fe^{2+}, Mg^{2+}). 1; Sample BG3. 2; Sample BP. 3; Sample AP5, Ca (X site) rich Elbaite. 4; Sample BPB, Cu containing Elbaite. 5; Sample AWB, Mn rich Elbaite.

BG1, BG2, BG3, and BG6) have 4~7 wt% of the sum of R^{2+} (Kim and Kim, 1993) and their characteristic feature is shown in near 3490 cm^{-1} in addition to near 3560 cm^{-1} peak. Hence, it can be deducible that near 3490 cm^{-1} peak is much affected by the contents of cation substituting Z site.

For the yellow elbaite, Li^{+} and Al^{3+} occupy Y sites. Two absorption bands have been identified at 3583 and 3483 cm^{-1} (Fig. 5). Absorption bands due to hydroxyl stretching vibration of analysed tourmalines are given in Table 4.

Both sections cut parallel and perpendicular to the c axis of sample BG2 and BG6 were prepared to illuminate difference of the stretching bands for two orientations of them. Sample BG2 shows absorption bands at 3495, 3551, 3572, 3651, and 3672. Absorption spectra // c axis is very much similar to ⊥ c axis showing slight different in intensities of absorption bands. But sample BG6 shows somewhat different absorption peak pattern between // c axis and ⊥ c axis in the region 3700~3630 cm^{-1} pertaining to O(1)H (Fig. 6).

Effect of thermal treatment

Different dehydroxylation mechanisms are

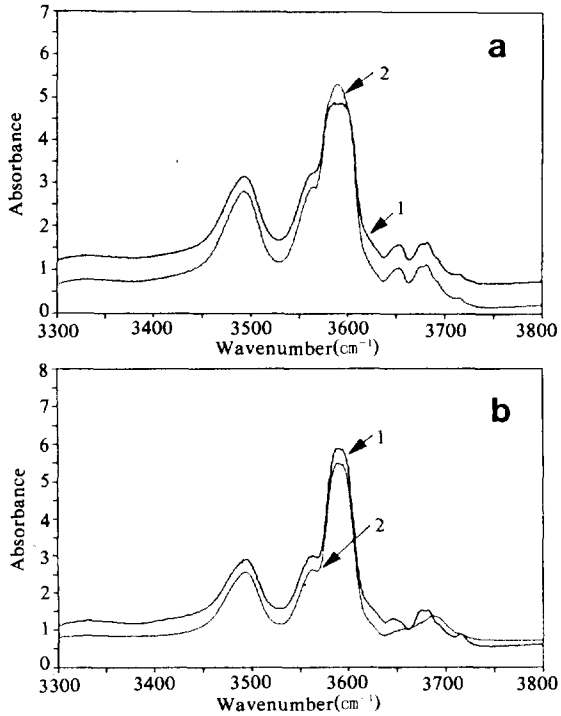

Fig. 6. Hydroxyl stretching region of IR spectrum of blue/green tourmaline minerals taken at two orientations. **(a)** Sample BG2, **(b)** Sample BG6. 1 // c axis, 2 ⊥ c axis.

operative in silicates depending on the presence or absence of the Fe^{2+} in the near environment of the OH group (Vedder and Wilking, 1969). In the first case the recombination of electron and protons cause the loss of OH groups and the simultaneous oxidation of iron at temperatures as low as 400 ℃, while in the second case the dehydroxylation is produced by condensation of two OH groups with the subsequent elimination of water. The temperature of dehydroxylation in this case can be higher than 1000 ℃ (Gonzalez-Carreno, 1988). On this basis, the study of dehydroxylation of tourmaline minerals can be used to identify the OH groups that are coordinated to Fe^{2+} ions.

The IR spectra of mono-colored tourmaline minerals, elbaite and schorl, at different temperatures are shown in Figure 7 and 8, respecti-

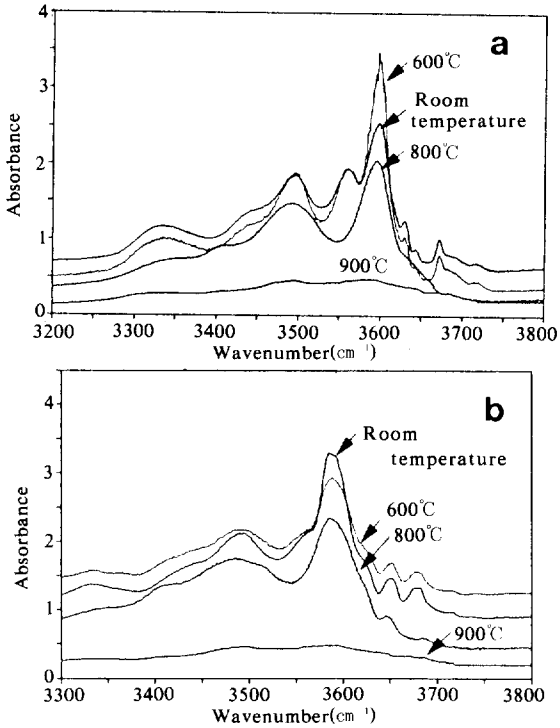

Fig. 7. Hydroxyl stretching region of IR spectrum of schorl samples heated in air at increasing temperature. **(a)** Sample BG1, **(b)** Sample BG4.

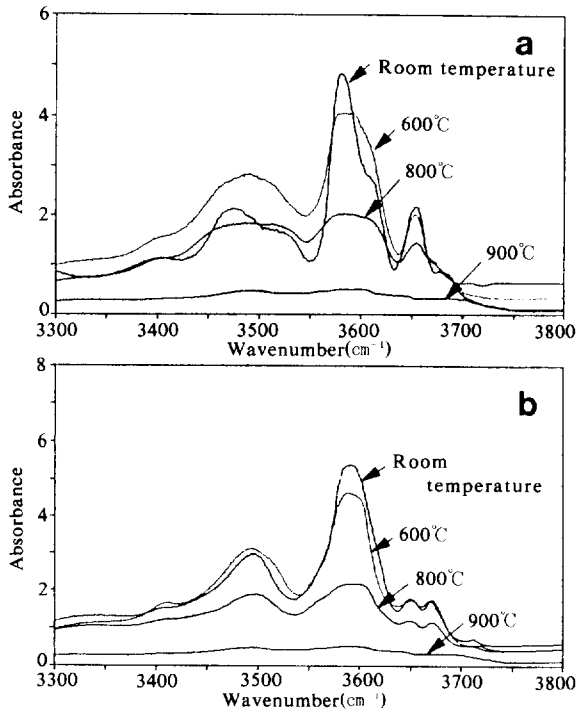

Fig. 8. Hydroxyl stretching region of IR spectrum of elbaite samples heated in air at increasing temperature. **(a)** Sample AGY, **(b)** Sample AW.

vely. No changes are observed in the absorption band except intensity below 600 ℃. However, at temperatures over 700 ℃, the dehydroxylation produces the continuous decrease in intensity of all the absorption bands. At 900 ℃ the complete dehydroxylation is achieved in all samples. In this process the two types of OH groups are lost, indicating that there is no considerable difference in the energy of stabilization for OH groups in the two structural sites. The comparison of spectra at different temperatures shows that, in the case of ferrous hydroxyl-bearing silicates, 3565 cm^{-1} peak appears, although it is not found in tourmalines having OH coordinated to other cations (Mn^{2+}, Cu^{2+}). It is observed that this peak persists up to 600 ℃, but completely disappears at 800 ℃ (Fig. 7). Gonzalez-Carreno, et al., (1988) reported that the temperature of dehydroxylation of OH coordinated to Fe^{2+} is 700~800 ℃, indicating that the migration of protons and electrons is hindered by the large distances existing between Y sites of contiguous Y_3OH_4 core units in tourmaline minerals.

All of the blue/green tourmaline minerals have Fe^{2+} according to the Mössbauer spectral study at room temperature. But at 800 ℃ the results of Mössbauer analyses show that Fe ions are ferric in all samples (Fig. 3). Therefore, it is interpreted that when Fe^{2+} is oxidized to Fe^{3+} upon heating, some of dehydroxylated OH groups may contribute to oxidation effects of Fe ions owing to protonation.

CONCLUSIONS

Mössbauer and Infrared absorption spectra of the iron-bearing tourmaline minerals show that the ferrous and ferric ions occupy the Y and Z

octahedral sites. The Fe ions are almost ferrous, predominantly partitioning into Y site and partly take in Z site. The Fe^{2+} contents of the Z sites in brownish black tourmaline minerals are higher than in blue/green tourmaline minerals. Therefore, 720 nm peak of brownish black samples is broader than that of blue/green tourmaline samples in optical spectra. All of the blue/green tourmaline minerals used in experiment have only Fe^{2+} ion.

IR spectra of mono-colored tourmaline minerals give information on the variation in the cation environments around OH groups. The differences of absorption spectra between O(1)H and O(3)H bonding are not detected in the heat-treated samples. But additional 3565 cm^{-1} peak appears in the case of ferrous hydroxyl bearing tourmaline, although it is not found in tourmaline having OH coordinated to other cations (Mg^{2+}, Mn^{2+}). The temperature of dehydroxylation for tourmaline having OH coordinated to Fe^{2+} is 700 ~800 ℃. Any change in peak intensity with different orientations is not found except certain samples which show somewhat different peak pattern 3700~3630 cm^{-1} pertaining to O(1)H.

REFERENCES

Barton, R. Jr. (1969) Refinement of the crystal structure of buergerite and the absolute orientation of tourmalines. Acta Crystallographica, B25, 1525-1533.

Burns, R. G. (1972) Mixed valencies and site occupancies of iron in silicate minerals from Mössbauer spectroscopy. Cannadian Journal of Spectroscopy, 17, 51-59.

Faye, G. H., Manning, P. G., Gosselin, J. R., and Tremblay, R. J. (1974) The optical absorption spectra of tourmaline: Importance of charge-transfer processes. Canadian Mineralogist, 12, 370-380.

Ferrow, E. A., Annersten, H., and Gunawardane, R. P. (1988) Mössbauer effect study on the mixed valence state of iron in tourmaline. Mineralogical Magazine, 52, 221-228.

Gonzalez-Carreno, T., Fernandez, M, and Sanz, J. (1988) Infrared and electron microprobe analysis of tourmalines. Physics and Chemistry of Minerals, 15, 452-460.

Gorelikova, N. V., Perfilyez, Y. D., and Bubeshkin, A. M. (1976) Mössbauer data on distribution of Fe ions in tourmaline. Zap Zses Mineral O -Va, 4:418-427 (transl. Int Geol Rev 20:982-990, 1978).

Hermon, E., Simkin, D. J., Donnay, G., and Muir, W. B. (1973) The distribution of Fe^{2+} and Fe^{3+} in iron-bearing tourmalines: A Mössbauer study. Tschermaks Mineralogische und Petrographische Mitteilungen, 19, 124-132.

Kim, H. J., and Kim, S. J. (1993) Chemical and Optical Absorption Spectroscopic Study of Colored Tourmalines. Journal of Mineralogical Society of Korea, 6, 1-16.

Korovshkin, V. V., Kuzmin, V. I., and Beloz, V. F. (1979) Mössbauer studies of structural features in tourmaline of various genesis. Physics and Chemistry of Minerals, 4, 209-220.

Mattson, S. M., and Rossman, G. R. (1984) Ferric iron in tourmaline. Physics and Chemistry of Minerals, 11, 225-234.

Rausell, F. A., Sanz, J., Fernandez, M., and Serratosa, J. M. (1979) Distribution of octahedral ions in phlogopites and biotites. In: Mortland MM and Farmer VC(ed) Development in Sedimentology 27. Elsevier, Amsterdam, 27-36.

Saegusa, N., Price, D. C., and Smith, G. (1978) Analysis of the Mössbauer spectra of several iron-rich tourmalines. Interantional conference of the application of the Mössbauer effect. Kyoto, Japan.

Saegusa, N., Price, D. C., and Smith, G. (1979) Mo ssbauer spectra of several iron-rich tourmalines (schorls). Journal of Physics (Paris), 40:C2/456-C2/459.

Sanz, J., Gc .ızalez-Carreno, T., and Gancedo, R. (1983) On dehydroxylation mechanisms of a biotite in vacuo and in oxygen. Physics and Chemistry of Minerals, 9, 14-18.

Simon, H. F. (1973) Near-infrared and Mössbauer study of cation site occupancies in tourmalines. Unpublished MS Thesis, MIT.

Smith, G. (1978) Evidence for absorption by exchange-coupled Fe^{2+} -Fe^{3+} pairs in the near infrared spectra of minerals. Physics and Chemistry of Minerals, 3, 375-383.

Strens, R. G. J. (1974) The common chain, ribbon and ring silicates. In: Farmer, V.C.(ed). The infrared spectra of minerals. Mineralogical Society Monography 4, Mineralogical Society. London. pp. 305-330.

Tsang, T. and Ghose, S. (1973) Nuclear magnetic resonance of ^{1}H, ^{7}Li, ^{11}B, ^{23}Na, and ^{27}Al in tourmaline (elbaite). American Mineralogist, 58, 224-229.

Vedder, W. (1964) Correlations between infrared spectrum and chemical composition of mica. American Mineralogist, 49, 736-768.

Vedder, W. and Wilkins, R. W. T. (1969) Dehydroxylation and rehydroxylation, oxidation and reduction of micas. American Mineralogist, 54, 482-509.

Wilkins, R. W. T., Farrell, E. F., and Naiman, C. S. (1969) The crystal field spectra and dichroism of tourmaline. Journal of Physics and Chemistry of Solids, 30, 43-56.